Progress In Electromagnetics Research, PIER 51, 153–165, 2005

ANALYSIS OF THE DOUBLE-NEGATIVE MATERIALS USING MULTI-DOMAIN PSEUDOSPECTRAL TIME-DOMAIN ALGORITHM

Y. Shi and C.-H. Liang

School of Electronic Engineering
Xidian University
Xi'an, Shaanxi 710071, P. R. China

Abstract—The increasing interest in electromagnetic effects in double-negative (DNG) materials requires a formulation capable of a full analysis of wave propagation in such materials. We develop a novel technique for discretization of the Drude medium model and adopt multi-domain pseudospectral time-domain (PSTD) algorithm and well-posed PML formulation to analysis the plane wave scattering properties of a single circular cylinder and a periodic array of the circular cylinders fabricated from the Drude medium. The simulation results show accuracy of the proposed constitutive equation-discretization scheme.

1. INTRODUCTION

It has been demonstrated recently, that a substance studied theoretically by Veselago [1] in which the dielectric constant ε and magnetic permeability μ are both negative, can be attained artificially in a metamaterial represented by a periodic medium of metallic wires [2] and split-ring resonators (SRR's) [3] that is characterized by an effective permittivity ε_{eff} and permeability μ_{eff} that can both have negative values in a certain frequency range. Remarkably, simultaneously negative material parameters lead to opposite directions of the Poynting and phase velocity vectors of plane waves propagating in the material, that is, to the existence of backward waves in double-negative (DNG) media. Three vectors $\vec{E}$, $\vec{H}$ and $\vec{k}$ form the left-handed triplets in DNG media, so such materials have been termed left-handed (LH) media.

Up to now both theoretical and experimental efforts [2–9] have focused on the study of the dispersion relations of the thin wire medium that is described by the frequency-dependent dielectric function

$$\varepsilon_{eff}(\omega) = 1 - \frac{\omega_p^2}{\omega^2} \tag{1}$$

Here ω_p is the plasma frequency, which depends on the geometrical parameters of the wires in a manner that allows scaling down ω_p to microwave frequencies. On the other hand, an array of split ring resonators exhibits behavior that can be described by an effective frequency-dependent permeability in the form

$$\mu_{eff}(\omega) = 1 - \frac{F\omega^2}{\omega^2 - \omega_0^2 + i\omega\Gamma} \tag{2}$$

Ziolkowski et al. [8] has enlivened the discussion by numerical simulation means. He chose the finite-difference time-domain (FDTD) method to solve Maxwell's equations directly, without any assumption on the sign of the refractive index or the direction of wave propagation inside the DNG slab. Davi et al. [9] add the perfectly matched layers (PMLs) formulation to Ziolkowski's approach to reduce the requirements for the computational domain, and simulate three-dimensional wave propagation problems.

In recent years, pseudospectral time-domain (PSTD) methods as an effective higher-order and spectral method have been proposed [10–16] and demonstrated to greatly outperform the FDTD method. The Fourier PSTD, originally proposed by Liu [10, 11], promises the superior accuracy in approximation of spatial derivatives by the fast Fourier transform (FFT) with a grid density of only two points per minimum wavelength. The Chebyshev PSTD [12–16] with Chebyshev collocation methods to approximate spatial derivatives has shown a spectral accuracy for discontinuous materials but with a slightly increased computational burden of π cells per minimum wavelength. With a multidomain scheme [12–16] that divides the whole computational domain into a series of subdomains naturally conformal to the problem geometry, Chebyshev PSTD method can deal with curved objects and strongly inhomogeneous media with a great flexibility.

In this paper, we develop a novel technique for discretization of the constitutive equations, and adopt the multidomain pseudospectral time-domain algorithm and well-posed PML formulation [17] to flexibly analyze plane wave scattering from an infinitely long cylinder fabricated from double-negative materials and one-dimensional periodical array composed of the cylinders fabricated from double-negative materials.

2. DISCRETE MODEL FOR MATERIAL EQUATIONS OF DNG CYLINDER

2.1. Maxwell's Equations in the Drude Materials

The formulation used to simulate wave scattering by an infinitely long cylinder fabricated from double-negative materials follows the one proposed by Ziolkowski et al. in [7]. There the authors developed the idea of the Drude medium used to simulate the negative ε and μ. Note that by simply imposing ε and μ negative inside the DNG slab would produce an unstable simulation, since the field at the interface, for a matched case, would blow up. Hence, the Drude medium approach is more general and can be applied to both matched and unmatched interfaces.

The constitutive relations for a frequency dispersive isotropic medium read as follows:

$$\begin{cases} \vec{D} = \varepsilon(\omega)\vec{E} \\ \vec{B} = \mu(\omega)\vec{H} \end{cases} \tag{3}$$

Negative permittivity and permeability are realized with the Lorentz medium model. The expressions for the permittivity and permeability are of the form

$$\begin{cases} \varepsilon(\omega) = \varepsilon_0 \left(1 + \dfrac{\omega_{pe}^2}{\omega_{oe}^2 - \omega^2 + j\Gamma_e \omega}\right) \\ \mu(\omega) = \mu_0 \left(1 + \dfrac{\omega_{pm}^2}{\omega_{om}^2 - \omega^2 + j\Gamma_m \omega}\right) \end{cases} \tag{4}$$

This model corresponds to a realization of DNG materials as mixtures of conductive spirals or omega particles, as discussed in [6]. Substituting those expressions into 2-D TM$_z$ (transverse magnetic to z) polarization Maxwell's equations in the frequency domain, we can obtain

$$\begin{aligned} j\omega H_x &= -\frac{1}{\mu_0}\frac{\partial E_z}{\partial y} - G_x \\ j\omega H_y &= \frac{1}{\mu_0}\frac{\partial E_z}{\partial x} - G_y \\ j\omega E_z &= \frac{1}{\varepsilon_0}\left(\frac{\partial H_y}{\partial x} - \frac{\partial H_x}{\partial y}\right) - S_z \end{aligned} \tag{5}$$

where

$$\begin{aligned} j\omega G_x &= \omega_{pm}^2 H_x - \Gamma_m G_x - \omega_{om}^2 F_x \\ j\omega F_x &= G_x \\ j\omega G_y &= \omega_{pm}^2 H_y - \Gamma_m G_y - \omega_{om}^2 F_y \\ j\omega F_y &= G_y \\ j\omega S_z &= \omega_{pe}^2 E_z - \Gamma_e S_z - \omega_{oe}^2 R_z \\ j\omega R_z &= S_z \end{aligned} \tag{6}$$

In the time domain, we finally have

$$\begin{aligned} \frac{\partial H_x}{\partial t} &= -\frac{1}{\mu_0}\frac{\partial E_z}{\partial y} - G_x \\ \frac{\partial H_y}{\partial t} &= \frac{1}{\mu_0}\frac{\partial E_z}{\partial x} - G_y \\ \frac{\partial E_z}{\partial t} &= \frac{1}{\varepsilon_0}\left(\frac{\partial H_y}{\partial x} - \frac{\partial H_x}{\partial y}\right) - S_z \end{aligned} \tag{7}$$

where

$$\begin{aligned}
\frac{\partial G_x}{\partial t} &= \omega_{pm}^2 H_x - \Gamma_m G_x - \omega_{om}^2 F_x \\
\frac{\partial F_x}{\partial t} &= G_x \\
\frac{\partial G_y}{\partial t} &= \omega_{pm}^2 H_y - \Gamma_m G_y - \omega_{om}^2 F_y \\
\frac{\partial F_y}{\partial t} &= G_y \\
\frac{\partial S_z}{\partial t} &= \omega_{pe}^2 E_z - \Gamma_e S_z - \omega_{oe}^2 R_z \\
\frac{\partial R_z}{\partial t} &= S_z
\end{aligned} \tag{8}$$

Note that with this new approach, we avoid the instability issue present when setting directly $\varepsilon < 0$ and $\mu < 0$. The application of multidomain PSTD algorithm is then straightforward, with G_x, F_x, G_y, F_y, S_z, and R_z being updated in each time step, as the $\vec{E}$ and $\vec{H}$ fields.

2.2. PML in the Drude Medium

Contrary to the two-time-derivative Lorentz material absorbing boundary condition [8] and Berenger's Split-PML [9] employed to terminate the grid, we adopt well-posed PML [15] to absorb the outgoing waves in this paper. Following [16], we introduce complex coordinate stretching variables as following:

$$\begin{cases} \partial x \Rightarrow \left[1 + \dfrac{\omega_x(x)}{j\omega}\right] \\ \partial y \Rightarrow \left[1 + \dfrac{\omega_y(y)}{j\omega}\right] \end{cases} \tag{9}$$

Defining new field variables for the PML region

$$\begin{cases} \tilde{H}_x = H_x + \omega_x Q_x \\ \tilde{H}_y = H_y + \omega_y Q_y \end{cases} \tag{10}$$

We can rewrite (7) and (8) for the PML as

$$\begin{aligned}
\frac{\partial \tilde{H}_x}{\partial t} &= -\frac{1}{\mu_0}\frac{\partial E_z}{\partial y} + (\omega_x - \omega_y)\left(\tilde{H}_x - \omega_x Q_x\right) - G_x - \omega_y F_x \\
\frac{\partial \tilde{H}_y}{\partial t} &= \frac{1}{\mu_0}\frac{\partial E_z}{\partial x} + (\omega_y - \omega_x)\left(\tilde{H}_y - \omega_y Q_y\right) - G_y - \omega_x F_y \\
\frac{\partial \tilde{E}_z}{\partial t} &= \frac{1}{\varepsilon_0}\left(\frac{\partial \tilde{H}_y}{\partial x} - \frac{\partial \tilde{H}_x}{\partial y}\right) - (\omega_x + \omega_y) E_z - \omega_x\omega_y P_z \\
&\quad -S_z - (\omega_x + \omega_y) R_z - \omega_x\omega_y R'_z
\end{aligned} \tag{11}$$

where

$$\begin{aligned}
\frac{\partial Q_x}{\partial t} &= \tilde{H}_x - \omega_x Q_x \\
\frac{\partial Q_y}{\partial t} &= \tilde{H}_y - \omega_y Q_y \\
\frac{\partial P_z}{\partial t} &= E_z \\
\frac{\partial G_x}{\partial t} &= \omega_{pm}^2 H_x - \Gamma_m G_x - \omega_{om}^2 F_x \\
\frac{\partial F_x}{\partial t} &= G_x \\
\frac{\partial G_y}{\partial t} &= \omega_{pm}^2 H_y - \Gamma_m G_y - \omega_{om}^2 F_y \\
\frac{\partial F_y}{\partial t} &= G_y \\
\frac{\partial S_z}{\partial t} &= \omega_{pe}^2 E_z - \Gamma_e S_z - \omega_{oe}^2 R_z \\
\frac{\partial R_z}{\partial t} &= S_z \\
\frac{\partial R'_z}{\partial t} &= R_z
\end{aligned} \tag{12}$$

Note that this nonsplit PML is well-posed for Lorentz medium because (10) remains the same symmetric hyperbolic system as the original Maxwell's equations plus some lower-order terms that do not affect the well-posedness [17]. When $\omega_{pe}^2 = \omega_{pm}^2 = 0$, the Maxwell's equations in PML region reduce to ones known for linear, nondispersive media. When $\omega_x = \omega_y = 0$, the PML equations reduce to Maxwell's equations for a regular Lorentz medium. In addition, (12) are ordinary differential equations without spatial derivatives, ensuring a simple and efficient implementation.

3. TIME STEPPING SCHEME

To advance (7) in time we use a fourth-order, fivestage, low-storage version of the classical Runge-Kutta method. For the equation

$$\frac{\partial q}{\partial t} = f(t, q) \tag{13}$$

we denote $q(t_n)$ as q_n and $t_n = n\Delta t$ where Δt is the time step size. The low-storage form of the Runge-Kutta method is given as [18]

$$\begin{array}{c} u_0 = q_n \\ q_{n+1} = u_n \end{array} \quad \forall j \in [1, 5] : \left\{ \begin{array}{r} k_j = a_j k_{j-1} + \Delta t f\left((n + c_j)\Delta t, u_{j-1}\right) \\ u_j = u_{j-1} + b_j k_j \end{array} \right. \tag{14}$$

where the constants a_j, b_j and c_j are determined to yield the desired order, $s-1$, of the scheme. For the scheme to be self-starting we require that $a_1 = 0$. Note that we need only two storage levels containing k_j and u_j to advance the solution. The actual values of a_j, b_j and c_j can be found in [18].

4. NUMERICAL RESULTS

The computational domain of rectangular shapes is divided into nonoverlapping quadrilaterals. The outer layer of quadrilaterals is used as PML subdomains in which the PML lossy media is applied using a quadratic profile of the PML absorption coefficient. Each quadrilateral is meshed with a grid where the grid points are located at the Chebyshev-Guass-Lobatto collocation points. In all examples, a grid with 16×16 points are used for each subdomain. The time function of the plane wave source and line electric current source is given by

$$f(t) = \left\{ \begin{array}{cc} g_{on}(t)\sin(\omega_0 t) & 0 \le t < mT_p \\ \sin(\omega_0 t) & mT_p \le t \le (m+n)T_p \\ g_{off}(t)\sin(\omega_0 t) & (m+n)T_p \le t \le (m+n+m)T_p \\ 0 & (m+n+m)T \le t \end{array} \right. \tag{15}$$

where $T_p = 1/f_0$ is the period of one single cycle and the three-derivative smooth window functions are given by

$$\left\{ \begin{array}{rcl} g_{on}(t) & = & 10x_{on}^3 - 15x_{on}^4 + 6x_{on}^5 \\ g_{off}(t) & = & 1 - \left(10x_{off}^3 - 15x_{off}^4 + 6x_{off}^5\right) \end{array} \right. \tag{16}$$

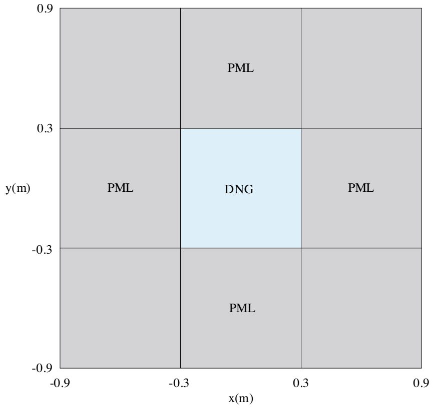

(a) Geometry and subdomains

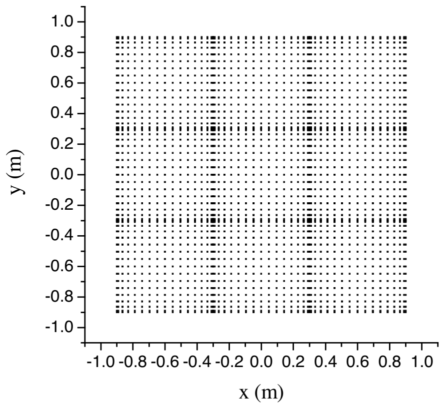

(b) grid point

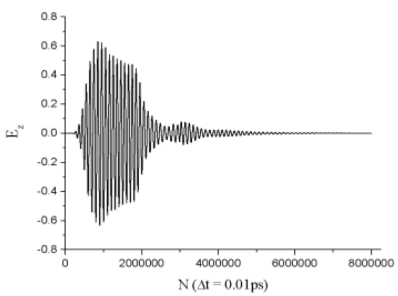

(c) E_z-field intensity at the center of the square cylinder

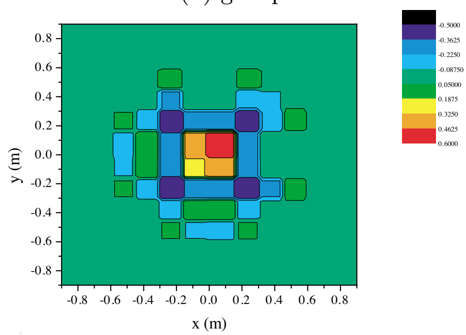

(d) E_z-field intensity distribution at time $t = 1000000\Delta t$.

Figure 1. Fields due to line source at the center of a square cylinder fabricated from DNG materials.

with

$$\begin{cases} x_{on} & = & 1 - (mT_p - t)/mT_p \\ x_{off} & = & (t - (m+n)T_p)/mT_p \end{cases} \tag{17}$$

The time function is the multiple cycle m-n-m pulse. It is a sinusoidal signal that has a smooth windowed turn-on for m cycles, a constant amplitude for n cycles, and then a smooth windowed turn-off for m cycles; hence, it has an adjustable bandwidth (through the total number of cycles $m+n+m$) centered at the frequency f_0. For the cases considered below, a 20-cycle, 5-10-5 pulse is used in computation. The Matrix-Pencil method [19] is used to reduce the required computing time to reach the harmonic steady state.

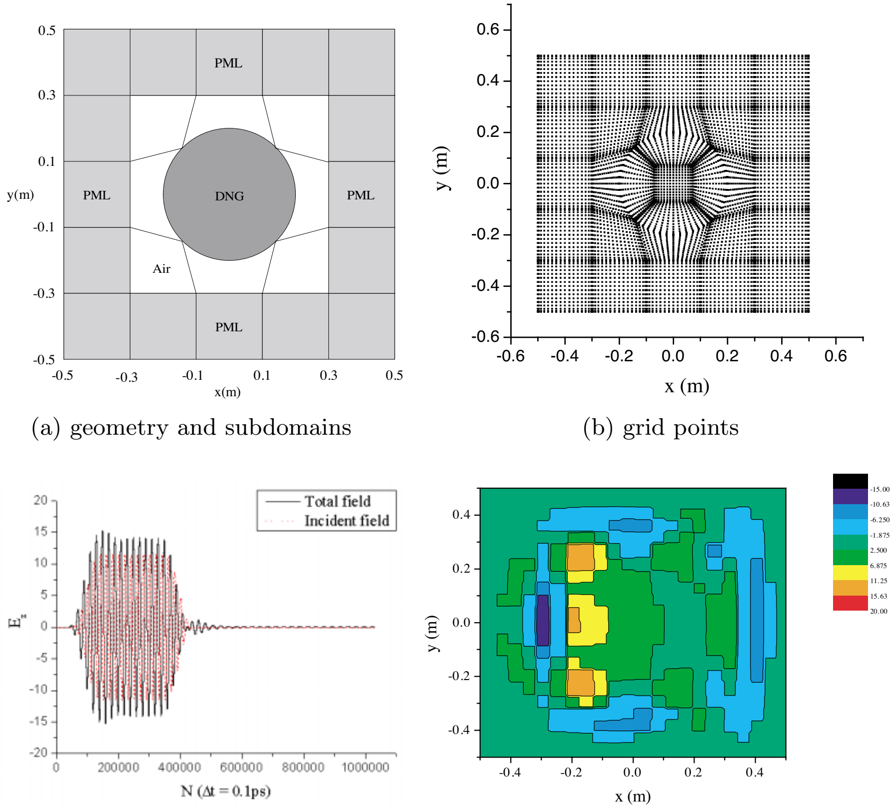

(a) geometry and subdomains

(b) grid points

(c) E_z-field intensity at $x = y = -0.210355\,\mathrm{m}$

(d) E_z-field intensity distribution at time $t = 250000\Delta t$

Figure 2. Plane wave scattering from a circular cylinder fabricated from DNG materials.

As a first example we consider a square cylinder fabricated from double-negative materials. The problem consists of an infinitely long line source located at the center of the square cylinder which is surrounded by free space, as shown Fig. 1(a). The grid points used in the calculation are shown in Fig. 1(b). The problem space is two-dimensional, with the electric field directed parallel to the line current. Hence, the field components H_x, H_y, E_z exist in the model. The peak of the incident spectrum is at $\omega_p = 5.0 \times 10^9\,\mathrm{rad/s}$, and the parameters in (4) are as follows: $\omega_{oe} = \omega_{om} = 1.0 \times 10^9\,\mathrm{rad/s}$, $\omega_{pe}^2 = \omega_{pm}^2 = 4.8 \times 10^{19}\,(\mathrm{rad/s})^2$, $\Gamma_e = \Gamma_m = 0$. With these choices, we obtain $\varepsilon(\omega)/\varepsilon_0 = \mu(\omega)/\mu_0$ for all ω and $\varepsilon(\omega)/\varepsilon_0 = \mu(\omega)/\mu_0 = -1$, at

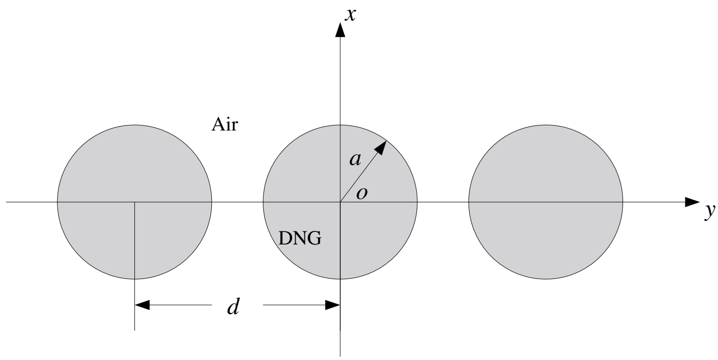

(a) a periodic array of the circular cylinders fabricated from DNG materials

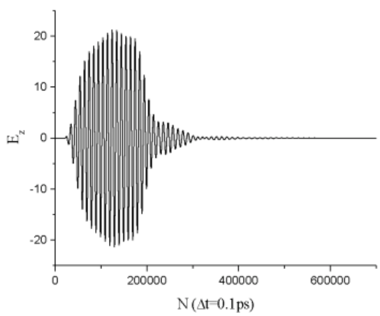

(b) E_z-field intensity at $x = y = -0.210355\,\mathrm{m}$

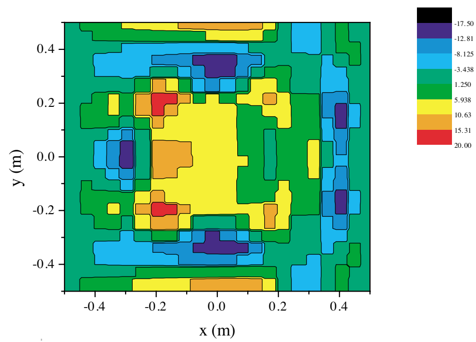

(c) E_z-field intensity distribution at time $t = 1250000\Delta t$

Figure 3. Plane wave scattering from a circular cylinder fabricated from DNG materials.

$\omega = \omega_p$. Fig. 1(c) illustrates the electric field intensity E_z at the center of the square cylinder, and Fig. 1(d) shows the E_z-field distribution corresponding to the time $t = 1000000\Delta t$.

The second example is the plane wave scattering from a circular cylinder fabricated from double-negative materials in free space. The radius of the cylinder is 0.2 m. The Fig. 2(a) illustrates the decomposition, and Fig. 2(b) shows the grid points used in the calculation. A plane wave is incident on the cylinder along the x-axis. The electric field intensity E_z at $x = y = -0.210355\,\mathrm{m}$ is shown in Fig. 2(c) and the E_z-field distribution corresponding to the time $t = 250000\Delta t$ is shown in Fig. 2(d).

As a final example, we consider the plane wave scattering from a periodic array of the circular cylinders fabricated from double-negative materials, as shown in Fig. 3(a). The parameters of the problem are $a = 0.2\,\mathrm{m}$ and $d = 1\,\mathrm{m}$. We apply the periodic boundary condition [20] into the multi-domain PSTD algorithm to calculate the electromagnetic fields. The geometry, grid points and source are similar to the second example [see Fig. 2(a) and (b)]. We also choose the observation point as $x = y = -0.210355\,\mathrm{m}$. Fig. 3(b) shows the electric field intensity E_z at the observation point, and Fig. 3(c) shows the E_z-field distribution corresponding to the time $t = 125000\Delta t$.

5. CONCLUSION

A complete formulation, adding the well-posed PML approach to the formulation of the Drude medium model, has been developed in this paper. The scattering properties of a single circular cylinder and a periodic array of the circular cylinders having both a dispersive permittivity and a dispersive permeability, in particular in the frequency range where both characteristics are negative, which corresponds to the case when cylinder exhibits the behavior of the double-negative medium, have been numerically studied. The simulation results show accuracy of the proposed constitutive equation-discretization scheme and provide a base for the more research on properties of the double-negative medium.

REFERENCES

1. Veselago, V. G., "The electrodynamics of substances with simultaneously negative values of ε and μ," *Sov. Phys. Usp.,* Vol. 10, 509–515, 1968.
2. Pendry, J. P., A. J. Holden, D. J. Robbins, and W. J. Stewart, "Low frequency plasmons in thin-wire structures," *J. Phys. Condens. Matter.,* Vol. 10, 4785–4809, 1998.
3. Pendry, J. P., A. J. Holden, D. J. Robbins, and W. J. Stewart, "Magnetism from conductors and enhanced nonlinear phenomena," *IEEE Trans. Microwave Theory Tech.,* Vol. MTT-47, 2075–2084, 1999.
4. Smith, D. R. and N. Kroll, "Negative refractive index in left-handed materials," *Phys. Rev. Lett.,* Vol. 85, 2933–2936, 2000.
5. Smith, D. R., D. C. Vier, W. Padilla, S. C. Nemat-Nasser, and S. Schultz, "Loop–wire medium for investigating plasmons at microwave frequencies," *Appl. Phys. Lett.,* Vol. 75, 1425–1427, 1999.

6. Tretyakov, S. A., I. S. Nefedov, C. R. Simovski, and S. I. Maslovski, "Advances in electromagnetics of complex media and metamaterials," *NATO-ARW Proceedings,* Kluwer, 2002.
7. Karkkainen, M. K. and S. I. Maslovski, "Wave propagation, refraction, and focusing phenomena in Lorentzian doublenegative materials: a theoretical and numerical study," *Microwave Opt. Technol. Lett.,* Vol. 37, 4–7, 2003.
8. Ziolkowski, R. W. and E. Heyman, "Wave propagation in media having negative permittivity and permeability," *Phys. Rev. E.,* Vol. 64, 2001.
9. Correia, D. and J. M. Jin, "3D-FDTD-PML analysis of left-handed metamaterials," *Microwave Opt. Technol. Lett.,* Vol. 40, 201–205, 2004.
10. Liu, Q. H., "The PSTD algorithm: A time-domain method requiring only two cells per wavelength," *Microwave Opt. Technol. Lett.*, Vol. 15, 158–165, 1997.
11. Tian, B. and Q. H. Liu, "Nonuniform fast cosine transform and chebyshev PSTD algorithm," *Progress in Electromagnetics Research*, PIER 28, 259–279, 2000.
12. Yang, B. and J. S. Hesthaven, "Multidomain pseudospectral computation of Maxwells equations in 3-D general curvilinear coordinates," *Appl. Numer. Math.,* Vol. 33, 281–289, 2000.
13. Fan, G.-X., Q. H. Liu, and J. S. Hesthaven, "Multidomain pseudospectral time-domain method for simulation of scattering from objects buried in lossy media," *IEEE Trans. Geosci. Remote Sens.,* Vol. GRS-40, 1366–1373, Jun. 2002.
14. Zhao, G. and Q. H. Liu, "The 3-D multidomain pseudospectral time-domain algorithm for inhomogeneous conductive media," *IEEE Trans. Antennas Propagat.,* Vol. AP-52, 742–749, Mar. 2004.
15. Fan, G. X. and Q. H. Liu, "A well-posed PML absorbing boundary condition for lossy media," *IEEE Antennas Propagation Soc. Int. Symp.,* Vol. 3, 2–5, 2001.
16. Chew, W. C. and W. H. Weedon, "A 3D perfectly matched medium from modified Maxwell's equation with stretched coordinates," *Microwave Opt. Technol. Lett.,* Vol. 7, 599–604, 1994.
17. Abarbanel, S. and D. Gottlieb, "A mathematical analysis of the PML method," *J. Comput. Phys.,* Vol. 134, 357–363, 1997.
18. Carpenter, M. H. and C. A. Kennedy, "Fourth order 2N-storage Runge-Kutta scheme," NASA, NASA-TM-109112, 1994.

19. Hua, Y. and T. K. Sarkar, "Generalized pencil-of-function method for extracting poles of an EM system from its transient response," *IEEE Trans. Antennas Propagat.,* Vol. AP-37, 229–234, Feb. 1989.
20. Taflove, A. and S. Hagness, *Computational Electrodynamics: The Finite-Difference Time-Domain Method,* Artech House, 2003.

Yan Shi was born in Tianjing, P. R. China on July 5, 1979. He received the Bachelor degree in Electromagnetic Field and Microwave Technology from Xidian University in 2001. Since 2002, he has been taking a combined master-doctor program and working for Ph.D. degree in Xidian University. His present research interests are mainly in computational electromagnetics and microstrip antenna.

Chang-Hong Liang was born in Shanghai, China on December 9, 1943. He graduated in 1965 from the former Xidian University, Xi'an, P. R. China, and continued his graduate studies until 1967. From 1980 to 1982, he worked at Syracuse University, New York, USA as a visiting scholar. He has been a professor and Ph.D. student advisor of Xidian University since 1986. Prof. Liang has wide research interests, which include computational microwave and computational electromagnetics, microwave network theory, microwave measurement method and data processing, lossy variational electromagnetics, electromagnetic inverse scattering, electromagnetic compatibility. He has received the titles "National Distinguished Contribution", "National Excellent Teacher", etc., Prof. Liang is a Fellow of CIE, a senior member of IEEE.